A correlative IR, MS, ^{1}H, ^{13}C and ^{15}N NMR and theoretical study of 4-arylthiazol-2(3*H*)-ones †

Kalevi Pihlaja,*[a] Vladimir Ovcharenko,[a] Erkki Kolehmainen,[b] Katri Laihia,[b] Walter M. F. Fabian,[c] Heinz Dehne,[d] Alexander Perjéssy,[f] Marion Kleist,[d] Joachim Teller[e] and Zora Šusteková[f]

[a] *Department of Chemistry, University of Turku, FIN-20014 Turku, Finland*
[b] *Department of Chemistry, University of Jyväskylä, FIN-40351 Jyväskylä, Finland*
[c] *Institute of Chemistry, Karl Franzens University, Heinrichstr. 28, A-8010 Graz, Austria*
[d] *Department of Chemistry, University of Rostock, Buchbinderstr. 9, D-18051 Rostock, Germany*
[e] *Micromod Partikeltechnologie GmbH, Friedrich-Barnewitz-Str. 4, D-18119 Rostock-Warnemünde, Germany*
[f] *Department of Organic Chemistry and Institute of Chemistry, Faculty of Natural Sciences, Comenius University, Mlynská dolina CH-2, SK-842 15 Bratislava, Slovak Republic*

Received (in Cambridge, UK) 17th July 2001, Accepted 21st November 2001
First published as an Advance Article on the web 11th January 2002

Sixteen 4-arylthiazol-2(3*H*)-ones (**3**) were synthesised by cyclisation of α-thiocyanatoacetophenones (**1**) in acid solution. They appear to prefer greatly the oxo tautomeric forms. In CCl_4 solution an equilibrium between the free C=O bond and a "dimeric" hydrogen-bonded form exists in which the latter predominates. Several IR and NMR (^{1}H, ^{13}C and ^{15}N) spectral properties are shown to correlate with Hammett σ-values and/or atomic Mulliken charges and bond orders, the latter being estimated by PM3 or AM1 semiempirical methods. The electron-impact mass spectra were also recorded and the fragmentation mechanisms interpreted in terms of the energetics of the ionic species. In addition, the geometric and electronic properties of 4-phenylthiazol-2(3*H*)-one (**3a**) and the related benzothiazol-2(3*H*)-one (**4**) based on *ab initio* HF/6-31 G* calculations are compared with each other.

Introduction

Thiazole derivatives like thiamine pyrophosphate and penicillin form very important classes of naturally occurring compounds.[1a] Certain 2-acylimino-4-thiazolines show significant activity as anticonvulsant agents[1b] and *N*-substituted benzothiazolinones stimulate plant growth.[1c] Annelated compounds like thiazolo[3,4-*a*]benzimidazoles possess reproducible *in vitro* anti-HIV activity.[1d] We also found that 3,4-diarylthiazolin-2-imines[1e] and dibromo derivatives of 4-substituted thiazol-2(3*H*)-ones exhibited fungicidal acitivities.[1f] Dhami *et al.*[1g] prepared several 4-arylthiazol-2(3*H*)-ones and found that some of them inhibited the growth of a wide variety of bacteria at a dilution of 1 : 1000.

Although it has already been proved by means of spectroscopic methods and HMO calculations that in solution the 2-oxo form is the predominant tautomer of thiazolinones,[1a] relatively little is known about the detailed electronic and structural characteristics of 4-arylthiazol-2(3*H*)-ones. Since they offer an interesting model system for molecular design of further biologically active compounds we decided to carry out a detailed spectroscopic (IR, NMR, MS), correlative and theoretical investigation of several 4-(substituted-phenyl) derivatives. The compounds studied (Scheme 1, **3a**–**p**) were prepared by cyclisation of α-thiocyanatoacetophenones (**1**) in acid solution.

The parent compound, 4-phenylthiazol-2(3*H*)-one (**3a**), was obtained by Dyckerhoff[2] and Arapides[3] *via* the above pathway. Other methods for preparation of **3** are known, such as the Hantzsch reaction of the corresponding α-bromoacetophenones with ammonium thiocarbamate in water at room temperature[4] or the reaction of α-(methoxycarbonyl)sulfenyl ketones with ammonium acetate in acetic acid at 80 °C.[5] The best synthetic route to compounds **3** still starts from α-thiocyanatoacetophenones (**1**), since this procedure is convenient and the yields of the purified products are high.

Results and discussion

Synthesis

We prepared **3** by a modification of the method used by Bariana *et al.*[6] and postulated the reaction to occur *via* the 2-amino-5-aryl-1,3-oxathiolium salt (**2**).[7,8]

IR Spectroscopy

Detailed infrared spectral data in dilute CCl_4 solutions for 4-arylthiazol-2(3*H*)-ones (**3**), except those[4] for **3a**, **3b**, **3e** and **3l**, have not been reported previously (Table 1). In concentrated $CHCl_3$ solutions the compounds exhibit a broad and rather complex absorption band in the region of 1680–1635 cm^{-1} belonging to the stretching vibration of the C=O group. On the other hand, in dilute CCl_4 solutions this absorption band is clearly split into two ν(C=O) maxima within the ranges of 1704–1695 cm^{-1} and 1661–1658 cm^{-1}. This is in accord with the results of Cornwell *et al.*,[4] who suggested that substituted thiazol-2(3*H*)-ones favour the oxo tautomer although in CCl_4 there exists an equilibrium between the free molecules and intermolecularly hydrogen bonded "dimeric" species (containing two hydrogen bonds, between the N–***H*** of one molecule and the C=***O*** of the other and *vice versa*) based on variable concen-

† Electronic supplementary information (ESI) available: NMR data, including graphs; Cartesian coordinates for **3a** and **4**. See http://www.rsc.org/suppdata/p2/b1/b106322g/

DOI: 10.1039/b106322g

Table 1 Characteristic IR spectral data (in cm^{-1}) for 4-arylthiazol-2(3*H*)-ones **3**

Compound	In $CHCl_3$ $\nu(C{=}O)_b$	In CCl_4 $\nu(C{=}O)_f$	In CCl_4 $\nu(C{=}O)_b$
3a	1658.8	1699.2[a]	1660.0[a]
3b	1660.3	1702.0[a]	1660.4[a]
3c	1657.6	1701.6	1658.4
3d	1661.2	1703.6	1660.8
3e	1659.6	1697.6[a]	1658.8[a]
3f	1667.6	1695.0	1658.8
3g	1668.8	1697.6	1659.6
3h	1659.8	1697.6	1658.8
3i	1660.0	1698.8	1659.6
3j	1658.8	1698.8	1659.2
3k	1658.4	1698.4	1659.2
3l	1657.6	1697.2[a]	1658.0[a]
3m	1657.6	1697.6	1658.0
3n	1635.2	1697.8	1658.5
3o	1661.1	—[b]	—[b]
3p	1678.6	—[c]	—[c]

[a] Values (in cm^{-1}) given in ref. 4 for concentrations of 10^{-2} mol dm^{-3} in CCl_4: **3a**, 1698, 1661; **3b**, 1697, 1662; **3e**, 1695, 1660; **3l**, 1694, 1659. [b] Insoluble in CCl_4; ν(C=O) 1648 cm^{-1} in Nujol.[4] [c] Insoluble in CCl_4.

tration experiments, *e.g.* on **3a**, **3b**, **3e** and **3l**. The corresponding $\nu(C{=}O)_f$ and $\nu(C{=}O)_b$ values in Table 1 are assigned to the vibrations of the free and hydrogen bonded molecules in analogy to Cornwell's work. It is evident that in concentrated $CHCl_3$ solutions the intermolecularly hydrogen bonded species ("dimeric" or those complexed with $CHCl_3$) are preferred. The wavenumbers for $\nu(C{=}O)_b$ vibrations in CCl_4 solutions are always lower, not very sensitive to substituents, and similar to those observed for the solid state spectra of a series of 4′-[bis(4-aryl-2-oxo-Δ^4-thiazolin-5-yl)methyl]benzo crown ethers,[9] which resemble compounds **3**. On the contrary the wavenumbers of $\nu(C{=}O)_f$ vibrations depend sufficiently on structural changes to be applicable in correlation analysis.[10] Attempts to obtain well distinguished absorption bands for the ring ν(N–H) stretching vibrations of the free species in dilute CCl_4 solutions were not successful, due to the very poor solubility of compounds **3** in apolar, aprotic and non-interacting solvents.

NMR Spectroscopy

For further structural characterisation of the studied compounds their ^{1}H (Table 2), ^{13}C (Table 3) and ^{15}N NMR chemical shifts (Table 4, for atom numbering of the compounds see Scheme 2) were recorded. In addition these data were used for correlations[10] with the calculated Mulliken charges and/or Hammett $\Sigma\sigma$ values[11] (see Correlation analysis). The H5 chemical shift shows the largest range (*ca.* 1 ppm), *i.e.* strongest substituent effects, which is also reflected in its correlations. The C2 carbon shifts do not vary very much (<1 ppm; no correlations either) but in general such a carbonyl carbon is fairly intact for substituent effects. Like H5, C5 is also most sensitive to substituent effects. The ^{15}N chemical shifts are very insensitive to substituent changes. The NH chemical shift of **3n** deserves a special mention since it is very broad and must be excluded from a $\Sigma\sigma$ correlation. This is obviously due to some kind of dynamic exchange between the NH and two OH protons in this compound.

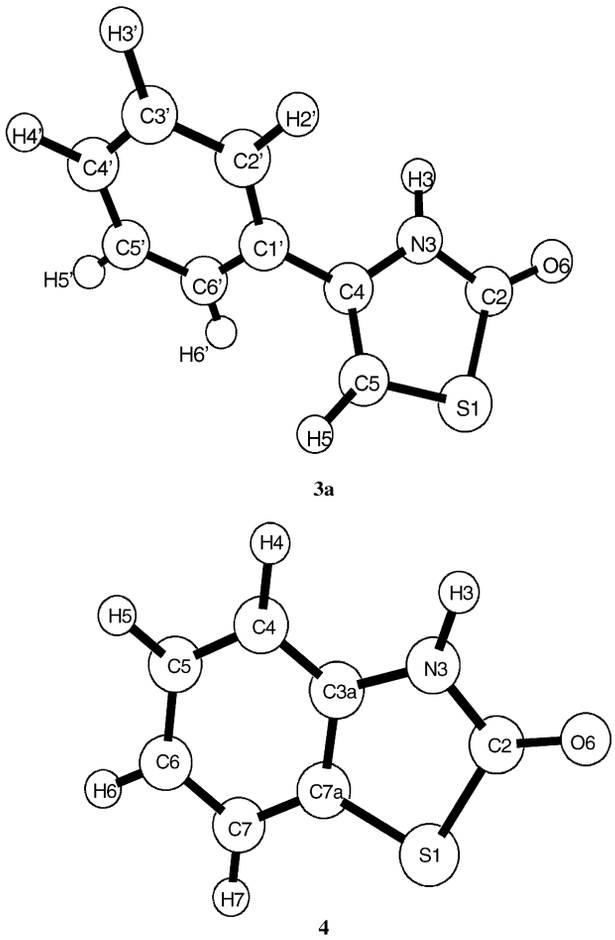

Scheme 2 Numbering of atoms in **3a** and benzothiazol-2(3*H*)-one (**4**). The structures were derived from HF/6-31G* calculations.

Mass spectrometry

According to our knowledge this is the first comprehensive treatment of the mass spectra of 4-arylthiazol-2(3*H*)-ones. Their $M^{+\bullet}$ ions are very stable under EI, giving rise to the base peaks in all the spectra except that of the *tert*-butyl-substituted compound **3k** (Table 5). The two most important fragmentation pathways are the losses of HNCO and (CO + CHS$^\bullet$) resulting in the $[M - HNCO]^{+\bullet}$ and $ArCNH^+$ ions, respectively. The

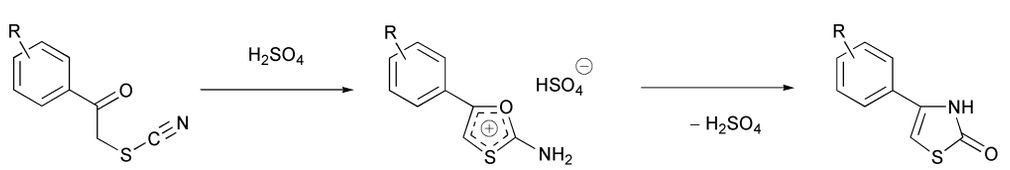

a: R = H, **b**: R = 4'-Br, **c**: R = 4'-Cl, **d**: R = 3',4'-Cl_2, **e**: R = 4'-CH_3, **f**: R = 2',4'-$(CH_3)_2$, **g**: R = 2',5'-$(CH_3)_2$, **h**: R = 3',4'-$(CH_3)_2$, **i**: R = 4'-C_2H_5, **j**: R = 4'-$CH(CH_3)_2$, **k**: R = 4'-$C(CH_3)_3$, **l**: R = 4'-OCH_3, **m**: R = 4'-OC_2H_5, **n**: R = 3',4'-$(OH)_2$, **o**: R = 4'-$NHCOCH_3$, **p**: R = 4'-NO_2

Scheme 1 Synthesis and structures of 4-arylthiazol-2(3*H*)-ones **3a**–**p**.

Table 2 ^{1}H NMR chemical shifts (δ/ppm) of 4-arylthiazol-2(3*H*)-ones **3**

Compd.	R	H-2′	H-3′	H-4′	H-5′	H-6′	H-5	NH	X
3a	H	7.66	7.40	7.33	7.40	7.66	6.73	11.76	—
3b	4′-Br	7.59	7.59	—	7.59	7.59	6.82	11.78	—
3c	4′-Cl	7.66	7.46	—	7.46	7.66	6.81	11.78	—
3d	3′,4′-Cl_2	7.90	—	—	7.60	7.60	6.96	11.83	—
3e	4′-CH_3	7.54	7.20	—	7.20	7.54	6.64	11.69	2.29[a]
3f	2′,4′-$(CH_3)_2$	—	7.10	—	7.06	7.21	6.22	11.43	2.32[b] 2.30[c]
3g	2′,5′-$(CH_3)_2$	—	7.17	7.13	—	7.15	6.26	11.42	2.29[d] 2.29[e]
3f	3′,4′-$(CH_3)_2$	7.45	—	—	7.15	7.36	6.64	11.61	2.23[f] 2.21[g]
3i	4′-C_2H_5	7.56	7.24	—	7.24	7.56	6.67	11.68	2.60[h] 1.17[i]
3j	4′-$CH(CH_3)_2$	7.57	7.26	—	7.26	7.57	6.66	11.65	2.88[j] 1.19[k]
3k	4′-$C(CH_3)_3$	7.58	7.40	—	7.40	7.58	6.63	11.73	1.26[l]
3l	4′-OCH_3	7.59	6.97	—	6.97	7.59	6.57	11.65	3.77[m]
3m	4′-OC_2H_5	7.57	6.95	—	6.95	7.57	6.57	11.64	4.03[n] 1.32[o]
3n	3′,4′-$(OH)_2$	7.03	—	—	6.78	6.93	6.36	9.5[p]	3.7[p]
3o	4′-$NHCOCH_3$	7.57	7.63	—	7.63	7.57	6.62	11.70	10.08[q] 2.06[r]
3p	4′-NO_2	7.91	8.26	—	8.26	7.91	7.21	12.05	—

[a] CH_3. [b] 2′-CH_3. [c] 4′-CH_3. [d] 2′-CH_3. [e] 5′-CH_3 [d(H-2′) < d(H-5′)]. [f] 3′-CH_3. [g] 4′-CH_3. [h] CH_2. [i] CH_3. [j] CH. [k] $(CH_3)_2$. [l] $C(CH_3)_3$. [m] OCH_3. [n] OCH_2. [o] CH_3. [p] Broad signals. [q] NH. [r] $COCH_3$.

Table 3 ^{13}C NMR chemical shifts (δ/ppm) of 4-arylthiazol-2(3*H*)-ones **3**

Compd.	R	C-1′	C-2′	C-3′	C-4′	C-5′	C-6′	C-4	C-5	C-2
3a	H	129.75	124.93	128.82	128.50	128.82	124.93	133.98	98.07	173.05
3b	4′-Br	128.81	126.82	131.69	121.62	131.69	126.82	132.79	99.10	172.79
3c	4′-Cl	128.48	126.58	128.79	133.04	128.79	126.58	132.74	99.02	172.81
3d[a]	3′,4′-Cl_2	129.97	126.58	131.82	130.86	130.86	124.81	131.50	100.70	172.63
3e[b]	4′-CH_3	127.03	124.81	129.34	138.06	129.34	124.81	133.99	97.01	173.03
3f[c]	2′,4′-$(CH_3)_2$	127.79	135.84	131.24	138.33	126.51	129.04	133.92	99.41	172.63
3g[d]	2′,5′-$(CH_3)_2$	130.38	132.86	130.48	129.66	134.93	129.45	133.98	99.62	172.54
3h[e]	3′,4′-$(CH_3)_2$	127.29	125.90	136.63	136.80	129.77	122.27	134.05	96.72	172.94
3i[f]	4′-C_2H_5	127.25	124.89	128.14	144.31	128.14	124.89	133.97	97.05	172.98
3j[g]	4′-$CH(CH_3)_2$	127.38	124.92	126.67	148.89	126.67	124.92	133.97	97.06	172.98
3k[h]	4′-$C(CH_3)_3$	127.02	124.67	125.51	151.09	125.51	124.67	133.93	97.09	173.02
3l[i]	4′-OCH_3	122.40	126.34	114.20	159.43	114.20	126.34	133.74	95.74	173.05
3m[j]	4′-OC_2H_5	122.25	126.32	114.61	158.70	114.61	126.32	133.75	95.64	173.04
3n	3′,4′-$(OH)_2$	121.66	112.86	145.64	146.35	115.90	116.91	134.59	95.07	173.43
3o[k]	4′-$NHCOCH_3$	124.45	125.48	119.03	139.62	119.03	125.48	133.83	96.66	173.14
3p	4′-NO_2	135.35	125.76	124.17	146.70	124.17	125.76	132.06	103.51	172.57

[a] Assignments of C-3′ and C-4′ verified. [b] CH_3 20.73 ppm. [c] 2′-CH_3 19.94 and 4′-CH_3 20.68 ppm. [d] 2′-CH_3 19.48 and 5′-CH_3 20.34 ppm. [e] 3′-CH_3 19.32 and 4′-CH_3 19.04 ppm. [f] CH_2 27.84 and CH_3 15.29 ppm. [g] CH 33.14 and $(CH_3)_2$ 23.58 ppm. [h] $\mathbf{C}(CH_3)_3$ 34.30 and $C(\mathbf{C}H_3)_3$ 30.88 ppm. [i] OCH_3 55.19 ppm. [j] OCH_2 63.15 and CH_3 14.51 ppm. [k] CO 168.60 and CH_3 24.12 ppm.

Table 4 ^{15}N NMR chemical shifts ($-\delta$/ppm from ext. CH_3NO_2) of 4-arylthiazol-2(3*H*)-ones **3**

Compound	NH	Other
3a	230.3	—
3b	230.9	—
3c	230.7	—
3d	231.2	—
3e	230.4	—
3f	225.2	—
3g	225.0	—
3h, **3i**, **3j**, **3k**	230.4	—
3l, **3m**	230.3	—
3n	229.5	—
3o	230.3	246.5 (NHCO)
3p	231.2	11.5 (NO_2)

metastable ion spectra show that the latter species are formed in two steps *via* the less stable $[M - CO]^{+\bullet}$ ions (*ca.* 5% RA). Apart from these main routes, there are numerous substituent-specific fragmentations of the $M^{+\bullet}$ ions, such as losses of the substituent (R = Me, Et, Cl, Br, NO_2), methyl losses from the $M^{+\bullet}$ ions bearing branched alkyl substituents (R = Pr^i and Bu^t), and rearrangement-accompanied losses of C_2H_4 (R = OEt) and CH_2CO (R = NHAc). The substituent-specific losses are only insignificant in the case of compounds **3l** and **3n** [R = OMe and 3,4-$(OH)_2$]. The characteristic fragmentations leading to the $[M - HNCO]^{+\bullet}$ and $ArCNH^+$ ions are often obscured by the substituent-specific fragmentations. Thus, peaks of $[M - HNCO]^{+\bullet}$ ions are absent from the spectrum of compound **3m** (R = OEt), but there are prominent peaks of $[M - C_2H_4 - HNCO]^{+\bullet}$ ions. Similarly, the $[M - C_2H_4 - COCHS]^+$ ions are three times more abundant than $[M - COCHS]^+$ ions. The $[M - NO_2 - COCHS]^+$ and $[M - COCHS]^+$ ions are of comparable abundance in the spectrum of compound **3c**. Formation of the abundant $[M - COCH_2]^{+\bullet}$ ions is followed by the usual HNCO and (CO + CHS) losses in the case of compound **3d**.

The mechanism of the HNCO and (CO + CHS) losses from the $M^{+\bullet}$ ions in the absence of substituent-specific fragmentations was deduced from quantum chemical calculations (PM3/UHF calculations, MOPAC 6.0,[12] see Computational details below) of the reaction profiles for various single-bond cleavages in the $M^{+\bullet}$ ions of compound **3a** (R = H). The calculations demonstrate that the $M^{+\bullet}$ ion of the oxo isomer $\mathbf{A_1}$ is thermodynamically by 68.6 kJ mol^{-1} more stable than the alternative hydroxy form **B** (Scheme 3). Moreover, the calculations predict the existence of yet another cyclic form of the $M^{+\bullet}$ ion, the four-membered **C**, which is less stable than the other two cyclic forms, but more stable than each of the open-chain forms $\mathbf{A_2}$ and $\mathbf{A_3}$ (Scheme 3). The most stable $M^{+\bullet}$ ($\mathbf{A_1}$) radical cation is practically flat, with both the phenyl and thiazole rings lying in the same plane. The C4–N and C5–S bonds are strengthened by aromatic conjugation, whereas the C2–N and C2–S bonds

Table 5 Main fragments in the 70-eV EI mass spectra of 4-arylthiazol-2(3*H*)-ones (**3**). The base peaks correspond to the $M^{+\bullet}$ ions unless specified otherwise

Compd.	R	$M^{+\bullet}$	$[M - H]^+$ or $[M - Me]^+$	$[M - CO]^{+\bullet}$	$[M - HNCO]^{+\bullet}$	$[M - COCHS]^+$ ($ArCNH^+$)	Ar^+ ($RC_6H_4^+$)	$[M - R]^+$	$[M - R - HNCO]^+$
3a	H	177	176(6)[a]	149(5)	134(19)	104(70)	77(26)	-—	—
3b	4′-Br	255(96) 257(100)	—	148(9)[c]	212(9) 214(8)	182(45) 184(45)	155(8) 157(8)	176(16)	—
3c	4′-Cl	211(100) 213(37)	—	148(4)[c]	168(16) 170(6)	138(71) 140(22)	111(15) 113(5)	176(16)	133(7)
3d	3′,4′-Cl_2	245(100) 247(67)	—	—	202(14) 204(9)	172(59) 174(38)	145(12) 147(8)	210(13), 212(5) 175(12) [M − 2Cl]	167(6) 169(4)
3e	4′-CH_3	191	176(12)[b]	163(3)	148(10)	118(54)	91(16)	[b]	147(12)[j]
3f	2′,4′-$(CH_3)_2$	205	190(30)[b]	176(4)[d]	162(6)[e]	132(29)	—	[b]	161(18)[j]
3g	2′,5′-$(CH_3)_2$	205	190(37)[b]	176(4)[d]	162(6)[f]	132(25)	—	[b]	161(14)[j]
3h	3′,4′-$(CH_3)_2$	205	190(17)[b]	—	162(9)[g]	132(38)	105(5)	[b]	161(5)[j]
3i	4′-C_2H_5	205	190(24)[b]	148(5)[c]	162(3)	132(32)	—	176(15)	147(15) [R = Me]
3j	4′-$CH(CH_3)_2$	219	204(75)[b]	—	—	146(12)	—	176(6)[i]	161(5) [R = Me]
3k	4′-$C(CH_3)_3$	233(90)	218(100)[b]	—	160(7)	—	—	—	—
3l	4′-OCH_3	207	206(6)[a], 192(6)[b]	—	164(8)[h]	134(44)	—	176(5)	149(16)
3m	4′-OC_2H_5	221	—	—	—	148(12), 120(38)*	121(9)	193(35) [M − C_2H_4]	—
3n	3′,4′-$(OH)_2$	209	208(4)[a]	181(3)	166(11)	136(45)	—	192(7)	—
3o	4′-$NHCOCH_3$	234	—	—	149(17)*	161(5), 119(38)*	92(6)*	192(64) [M − $COCH_2$]	—
3p	4′-NO_2	222	—	148(6)[c]	—	149(26), 103(21)*	76(13)*	176(11)	—

[a] $[M - H]^+$. [b] $[M - Me]^+$. [c] $[M - R - CO]^+$. [d] $[M - H - CO]^+$. [e] Doublet comprising *ca.* 60% of $[M - Me - CO]^+$ ions. [f] Doublet comprising *ca.* 70% of $[M - Me - CO]^+$ ions. [g] Doublet comprising *ca.* 40% of $[M - Me - CO]^+$ ions. [h] Doublet comprising *ca.* 30% of $[M - Me - CO]^+$ ions. [i] Doublet comprising *ca.* 20% of $[M - Me - CO]^+$ ions. [j] $[M - H - HNCO]^+$. * Following the loss of either $COCH_2$ (**3o**), C_2H_4 (**3m**), or NO_2 (**3p**) from the $M^{+\bullet}$. For instance: *m/z* 149 is $[M - COCH_2 - HNCO]^{+\bullet}$ in (**3o**), *etc*.

Table 6 Selected PM3 and AM1 semiempirical data (Mulliken charges and populations) for compounds **3**[a]

Compound	*p*(C2=O6)/AM1	*q*(C4)/PM3	*q*(C5)/PM3	*q*(C1′)/PM3	*q*(C2′/6′)/AM1	*q*(N3)/AM1	*q*(C3′/5′)/AM1
3a	1.8181	−0.0555	−0.4674	−0.0508	−0.1664[b]	−0.4503	−0.1903[b]
3b	1.8224	−0.0635	−0.4622	−0.0427	−0.1683[b]	−0.4499	−0.1537[b]
3c	1.8212	−0.0591	−0.4645	−0.0514	−0.1588[b]	−0.4502	−0.1768[b]
3d	1.8234	−0.0635	−0.4612	−0.0353	−0.1488[c]/−0.1613[d]	−0.4498	−0.0719[c]/−0.1687[d]
3e	1.8172	−0.0518	−0.4695	−0.0597	−0.1610[b]	−0.4505	−0.1876[b]
3f	1.8161	−0.0514	−0.4677	−0.0694	−0.0578[c]/−0.1513[d]	−0.4492	−0.1869[c]/−0.1947[d]
3g	1.8164	−0.0541	−0.4669	−0.0546	−0.0680[c]/−0.1527[d]	−0.4489	−0.1853[c]/−0.0956[d]
3h	1.8165	−0.0513	−0.4697	−0.0543	−0.1567[c]/−0.1662[d]	−0.4505	−0.0866[c]/−0.1822[d]
3I	1.8171	−0.0516	−0.4696	−0.0597	−0.1626[b]	−0.4505	−0.1847[b]
3j	1.8172	−0.0522	−0.4693	−0.0571	−0.1635[b]	−0.4505	−0.1829[b]
3k	1.8169	−0.0514	−0.4696	−0.0583	−0.1640[b]	−0.4505	−0.1841[b]
3l	1.8174	−0.0447	−0.4721	−0.0946	−0.1294[b]	−0.4515	−0.2382[b]
3m	1.8171	−0.0437	−0.4726	−0.0972	−0.1286	−0.4515	−0.2406[b]
3n	1.8163	−0.0510	−0.4711	−0.0453	−0.1664[c]/−0.1623[d]	−0.4497	+0.0746[c]/−0.2262
3o	1.8180	−0.0531	−0.4664	−0.0666	−0.1351[b]	−0.4516	−0.2312[b]
3p	1.8321	−0.0874	−0.4465	−0.0196	−0.1843[b]	−0.4490	−0.1226[b]

[a] Numbering of atoms, see Scheme 2. [b] Results from Boltzmann averaging (room temperature) of the calculated differences over the possible orientations of the substituents; NMR shifts are the same due to rapid rotation. [c] In the case of compounds substituted at C3′, C3′ and C5′ are not equivalent and show distinct NMR signals; therefore *q*-values for these atoms are listed separately (since the shifts are separate they are to be used as separate entries in the correlations). [d] In the case of compounds substituted at C2′, C2′ and C6′ are not equivalent and show distinct NMR signals; therefore *q*-values for these atoms are listed separately (since the shifts are separate they are to be used as separate entries in the correlations).

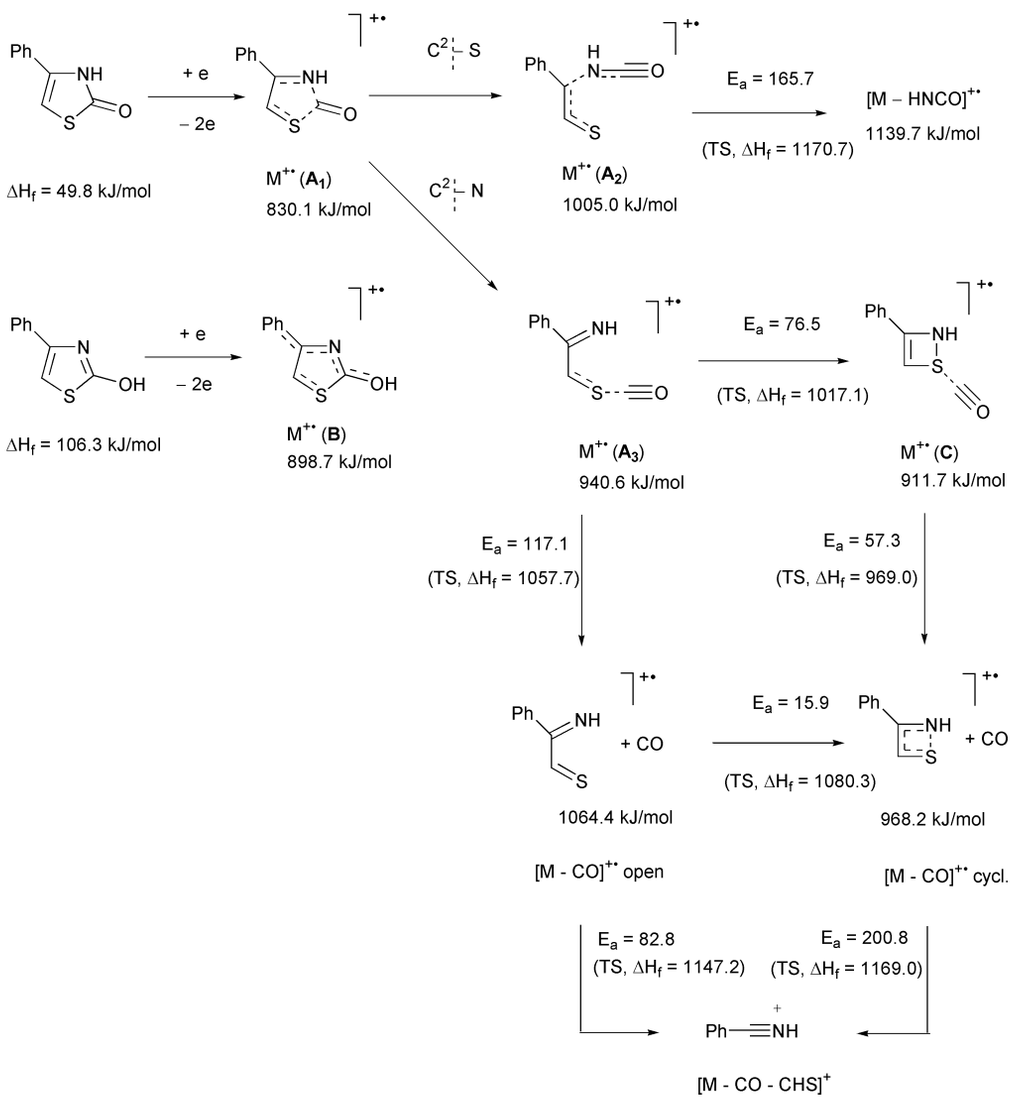

Scheme 3 Energy barriers for unimolecular decompositions (E_a, kJ mol^{-1}) approximated as differences between the calculated enthalpies of formation (PM3/UHF) at 298 K for the transition states (TS) and the parent ion for **3a**.

are weakened, which results in the facile ring opening and subsequent loss of the CO and HNCO fragments (Scheme 3).

An analysis of the isomeric $M^{+\bullet}$ structures produced by the alternative bond cleavages in $M^{+\bullet}$ ($\mathbf{A_1}$) suggests that the initial cleavage of the C2–S bond should result in the HNCO loss, whereas the $M^{+\bullet}$ fragmentation initiated by the C2–N bond cleavage is more likely to involve the consecutive losses of CO and CHS$^{\bullet}$ (possibly *via* the four-membered cyclic isomer **C**).

Table 7 Comparison of selected HF/6-31G* *ab initio* theoretical data[a] and wavenumbers of C=O stretching vibrations for compound **3a** and related benzothiazol-2(3*H*)-one **4**[b]

Data	Compound **3a**		Compound **4**	
Total atomic charges	O6	−0.5815	O6	−0.5751
	C2	0.5790	C2	0.5862
	N3	−0.8262	N3	−0.8613
	C4	0.3837	C3a	0.3962
	C5	−0.5079	C7a	−0.2715
	S1	0.2453	S1	0.2707
Overlap populations	C2–O6	0.5744	C2–O6	0.5766
	C2–N3	0.2450	C2–N3	0.2483
	N3–C4	0.2670	N3–C3a	0.2276
	C4–C5	0.6428	C3a–C7a	0.5508
	C5–S1	0.2278	C7a–S1	0.2139
	S1–C2	0.3491	S1–C2	0.3382
Bond lengths/Å	C2–O6	1.207	C2–O6	1.205
	C2–N3	1.374	C2–N3	1.373
	N3–C4	1.398	N3–C3a	1.390
	C4–C5	1.328	C3a–C7a	1.385
	C5–S1	1.751	C7a–S1	1.759
	S1–C2	1.781	S1–C2	1.786
Bond angles/°	S1–C2–N3	107.4	S1–C2–N3	108.5
	C2–N3–C4	116.5	C2–N3–C3a	116.8
	N3–C4–C5	112.7	N3–C3a–C7a	112.2
	C4–C5–S1	112.3	C3a–C7a–S1	111.1
	C5–S1–C2	91.1	C7a–S1–C2	91.3
Wavenumbers/cm^{-1}				
Calculated	ν(C2=O6)	1763	ν(C2=O6)	1772
Experimental/CCl_4	$\nu(C2=O6)_f$	1699.2	$\nu(C2=O6)_f$	1713.6[c]

[a] Only the data characterising the five-membered rings were selected. [b] For numbering of atoms see Scheme 2. [c] Taken from ref. 13.

Indeed, the calculated length of the C–N bond connecting the emerging HNCO fragment in the open-chain $M^{+\bullet}$ ($\mathbf{A_2}$) ion is larger (1.46 Å) than that of the other C–N bond (1.35 Å) which should be cleaved to produce the $[M - CO]^{+\bullet}$ ion from $M^{+\bullet}$ ($\mathbf{A_2}$). A transition state for the loss of HNCO from the $M^{+\bullet}$ ($\mathbf{A_2}$) structure was found to be 166 kJ mol^{-1} higher in energy than the parent ion. The search for a TS corresponding to the loss of CO from $M^{+\bullet}$ ($\mathbf{A_2}$) did not converge to a saddle point. On the other hand, each of the C–S bonds connecting CO fragments in the $M^{+\bullet}$ ($\mathbf{A_3}$) and $M^{+\bullet}$ (**C**) forms is quite weak (1.84 and 1.93 Å, respectively). The four-membered cyclic isomer of the $[M - CO]^{+\bullet}$ ion is more stable than its open-chain counterpart (Scheme 3), which would easily cyclise into the former (the predicted energy of activation is only *ca.* 16 kJ mol^{-1}). The lowest-energy fragmentation path thus leads to the cyclic isomer of $[M - CO]^{+\bullet}$, although the subsequent loss of CHS$^{\bullet}$ occurs more easily from the open form of $[M - CO]^{+\bullet}$ (Scheme 3). The enthalpies of formation of the systems ($PhC_2HS^{+\bullet}$ + HNCO) and ($PhCNH^{+}$ + $^{\bullet}$CHS) are similar, therefore the much greater abundance of the $[M - CO - CHS]^{+}$ ions compared to that of $[M - HNCO]^{+\bullet}$ in the spectrum of **3a** (70% *vs.* 19% RA, Table 5) can be explained by the higher energy of activation for the HNCO cleavage from $M^{+\bullet}$ ($\mathbf{A_2}$) (Scheme 3).

Theoretical data

From the values obtained by semiempirical quantum chemical methods, the Mulliken C=O bond orders of compounds **3** [*p*(C2=O6)] and the Mulliken charges at C1′, C2′/6′, C3′/5′, C4, and C5 carbon atoms (*q*-values) derived by the PM3 method [C1′, C4, and C5] and those derived by the AM1 method [C2′–C6′] were selected as the most consistent for linear correlations with spectral data.[10] As to the Mulliken nitrogen atom charges [*q*(N3)], the AM1 data appeared most suitable. These selected semiempirical theoretical data are listed in Table 6.

In principle, for disubstituted derivatives two conformations as defined by the torsional angle N3–C4–C1′–C2′ (see Scheme 2 for numbering of atoms) are possible. The energy differences between these two conformations are very small. However, even for derivatives unsubstituted at carbon atoms C2′ and C6′ or C3′ and C5′, respectively, the corresponding Mulliken charges are different. Consequently, for the correlation analyses a Boltzmann weighting on the calculated energy differences of the possible conformations at room temperature was done for the Mulliken charges.

For comparison Table 7 lists selected theoretical data based on an HF/6-31G* *ab initio* approach and the calculated and experimental wavenumbers for the C=O stretching vibration for compound **3a** and the related benzothiazol-2(3*H*)-one **4**. Compound **4** is a condensed aromatic analogue of thiazol-2(3*H*)-one or its derivatives **3** and its spectral properties, interactions with solvents and hydrogen bonding ability have been recently thoroughly studied.[13,14] The comparison shows that compound **4** exhibits a $\nu(C=O)_f$ absorption band which is 14.4 cm^{-1} higher than that of compound **3a**. This is in good accord with the calculated *ab-initio* C2–O6 overlap population of **4**, which is higher than the corresponding overlap population of **3a**, whereas the total negative charge at O6 as well as the corresponding C2–O6 bond length for **4** are smaller than those for **3a**. Based on the bond angles for **3a** and **4** it is evident that no significant difference is caused by the possible change in the strain of the five-membered ring due to annelation. Finally the overlap populations over the bonds of the five-membered 2(3*H*)-thiazole ring show that in the case of **3a** the system is significantly enriched by electrons, which are obviously well conjugated with the carbonyl group which causes a decrease in the $\nu(C=O)_f$ band position ($\Delta\nu$ = 14.4 cm^{-1}) against the benzothiazolinone analogue **4**. This decrease is in good agreement with the calculated difference of the ν(C=O) values ($\Delta\nu$ = 9 cm^{-1}).

Table 8 Correlation analysis ($y = ax + b$) of selected spectral data for compounds **3a**.[a] p refers to the Mulliken AM1 bond orders and q to the AM1 or PM3 charges

y	x	N[b]	a	b	R[c]	s[d]	p[e]
ν(C2=O6)$_f$/CCl$_4$	$\Sigma\sigma$	13[f]	7.32 ± 0.44	1699.5	0.981	0.42	<0.0001
ν(C2=O6)$_f$/CCl$_4$	p(C2=O6)/AM1	13[f]	812.8 ± 67.5	221.1	0.964	0.57	<0.0001
δH2′	$\Sigma\sigma$	13[g]	0.35 ± 0.05	7.62	0.914	0.06	<0.0001
δH3′	$\Sigma\sigma$	13	1.04 ± 0.13	7.40	0.926	0.14	<0.0001
δ(^{13}C2′/6′)	q(C2′/6′)/AM1	19[g]	81.6 ± 12.6	138.7	0.843	1.7	<0.0001
	q(C2′/6′)/PM3	19[g]	67.8 ± 10.6	136.8	0.840	1.8	<0.0001
δ(^{13}C3′/5′)	q(C3′/5′)/AM1	21	86.5 ± 13.3	141.9	0.830	4.3	<0.0001
	q(C3′/5′)/PM3	21	83.9 ± 13.6	142.2	0.817	4.4	<0.0001
δH3′/5′	q(C3′/5′)/AM1	16[h]	10.5 ± 1.44	9.26	0.890	0.16	<0.0001
	q(C3′/5′)/PM3	16[h]	8.83 ± 0.21	7.88	0.896	0.16	<0.0001
δH5′	$\Sigma\sigma$	15	0.92 ± 0.15	7.34	0.863	0.19	<0.0001
δH5	$\Sigma\sigma$	16	0.64 ± 0.10	6.67	0.865	0.13	<0.0001
	$\Sigma\sigma$	13[j]	0.50 ± 0.05	6.72	0.958	0.05	<0.0001
δH5	q(C5)/AM1	13[j]	37.4 ± 1.7	37.4	0.989	0.03	<0.0001
	q(C5)/AM1	16	42.0 ± 10.2	29.1	0.739	0.17	=0.00107
	q(C5)/PM3	13[j]	25.6 ± 2.0	18.7	0.967	0.05	<0.0001
δNH	$\Sigma\sigma$	13[j]	0.30 ± 0.04	11.73	0.914	0.05	<0.0001
δ(^{13}C4)	q(C4)/AM1	15[k]	62.5 ± 12.8	129.1	0.805	0.40	=0.00030
	q(C4)/PM3	15[k]	51.5 ± 10.2	136.5	0.813	0.39	=0.00023
δ(^{13}C4)	$\Sigma\sigma$	16	−2.30 ± 0.25	133.4	−0.924	0.33	<0.0001
δ(^{13}C5)	q(C5)/AM1	16	313.7 ± 39.5	244.3	0.905	0.96	<0.0001
	q(C5)/PM3	16	440.0 ± 64.2	332.8	0.878	1.08	<0.0001
δ(^{13}C5)	$\Sigma\sigma$		6.06 ± 0.55	97.8	0.957	0.66	<0.0001
δ(^{13}C1′)	q(C1′)/AM1	15[g]	139.8 ± 10.7	135.4	0.964	0.90	<0.0001
	q(C1′)/PM3	15[g]	152.1 ± 17.2	136.5	0.926	1.27	<0.0001
δ(^{15}N3)	$\Sigma\sigma$	13[j]	0.91 ± 0.09	230.5	0.950	0.11	<0.0001
δ(^{15}N3)	q(N3)/AM1	13[j]	377.1 ± 74.7	400.5	0.836	0.19	=0.00037
	q(N3)/PM3	13[j]	232.5 ± 57.9	234.4	0.771	0.23	=0.00203

[a] For numbering of atoms see Scheme 2. [b] Number of compounds used in correlation (see also the last paragraph before computational details). [c] Correlation coefficient. [d] Standard deviation. [e] p-value for the correlation. [f] Data for **3f** excluded, no IR-data obtained for **3o** and **3p** (see Table 2). [g] Data for **3n** excluded. [h] Data for **3o** excluded. [j] Data for **3f**, **3g** and **3n** are excluded. [k] Data for **3d** excluded.

Correlation analysis

The statistical correlations of IR and NMR spectral data with Hammett σ constants[11] of substituents R (or in fact with their sums, $\Sigma\sigma$ for disubstituted compounds) and with some PM3 and AM1 theoretical data for compounds **3** are given in Table 8.[10] The ν(C=O)$_f$ wavenumbers exhibit significant linear correlations with both Hammett σ values and Mulliken AM1 C=O bond orders (p). The relatively high value of the slope (a = 7.32 cm^{-1}) of ν(C=O)$_f$ *vs.* $\Sigma\sigma$ correlation suggests a very efficient transmission of electronic effects from the 4-aryl moiety to the terminal carbonyl group attached to the 2(3*H*)-thiazole ring.

Satisfactory or good correlations can be found also between the ^{13}C NMR chemical shifts of C1′, C2′/6′, C3′/5′, C4, and C5 carbon atoms and the corresponding Mulliken AM1 and PM3 charges (q; Table 8). The relatively large value of the slope (a = 313.7 ppm/AM1 or 440.0 ppm/PM3) of the δ(^{13}C5) *vs.* q(C5) correlation indicates the high sensitivity of C5 to substituent effects, which evidently plays a significant role in the transmission of electronic effects from the 4-aryl moiety to the C=O group and indicates that it takes place *via* the C5 atom. Similarly the C1′, C2′/6′, C3′/5′, and C4 carbon chemical shifts show a good or at least a satisfactory correlation with the AM1 and PM3 Mulliken charges and those of C4 and C5 also with the $\Sigma\sigma$ values (Table 8).

Several ^{1}H chemical shifts (those of H2′, H3′, H5′, H5 and NH) show a good or fair correlation with the Hammett constants and in the case of H3′/5′ and H5 also with the AM1 and PM3 Mulliken charges of the respective carbon atoms (Table 8). Despite the fact that the ^{15}N chemical shifts of the ring NH of compounds **3a**–**p** exhibit a very narrow range (−230.5 ± 1.0 ppm), *i.e.* they show very weak substituent dependences, the shifts (measured within ±0.1 ppm) do correlate with both of the above parameters (see below) excluding the 3,4-dihydroxy **3n** (due to intramolecular hydrogen bonding) and the *o*-methyl substituted derivatives **3f** and **3g**, of which the latter two show a very clear *ortho*-effect (δ_N = 225.1 ± 0.1 ppm). It is worth emphasizing that the latter three compounds (**3f**, **g**, **n**) appear to behave exceptionally since omitting them from several correlations significantly improved the fits. For instance, in the case of the H5 *vs.* q(C5)/AM1 correlation the plot with all shifts has R = 0.739 whereas that excluding the above compounds has R = 0.989 (Table 8). This was more or less in line with the expectations.

One should note that usually the number of correlated parameters is 16 (equal to the number of compounds; Table 8) but less as stated above owing to some omissions or to the fact that some of the positions are substituted (proton chemical shifts). In the case of carbons the Mulliken AM1 charges are different for C2′ and C6′ or C3′ and C5′ if some of these positions are substituted. Therefore in these cases the number of correlated parameters can be higher than 16 (up to 21).

Computational details

Molecular structures were calculated by the semiempirical AM1[15] and PM3[16] Hamiltonians using the VAMP 4.40 program package.[17] Geometries were completely optimised by the eigenvector (EF) following routine[18] without any restriction and using the PRECISE option. In addition, for compounds **3a** and **4** *ab initio* HF/6-31G* computations using the Gaussian 94 program suite[19] were performed. Calculated frequencies are scaled by a factor 0.8929.[20]

Unimolecular decompositions of gas-phase ionic species formed from **3a** under EI were calculated by the PM3 method[16] using the MOPAC 6.0 program[12] with the PRECISE option and the unrestricted Hartree–Fock (UHF) open-shell approximation. Transition-state structures were located using either TS or NLLSQ routines and characterised by force calculations (FORCE routine) to verify that they had one, and only one, negative force constant (imaginary frequency). The energy barriers (E_a) for the unimolecular decompositions shown in Scheme 3 correspond to differences between the calculated standard enthalpies of formation ($\Delta H_f^{298\ K}$, MOPAC standard

output) of the transition state structures and respective parent ions.

Experimental

Preparation of 4-arylthiazol-2(3*H*)-ones (3)[7]

The corresponding α-thiocyanatoacetophenone (0.1 mol) was dissolved in glacial acetic acid (10 ml), 50% sulfuric acid (2 ml) was added and then the mixture was heated to boiling for 10 min. The products **3** crystallised or had to be precipitated by water. They were collected on suction and recrystallised from ethanol–acetone.

Infrared spectra

The IR spectra were measured at room temperature in the region of 1750–1600 cm^{-1} using a Zeiss Specord M 80 spectrometer. The measurements were carried out in $CHCl_3$ and CCl_4 employing NaCl cells of 1 mm and 10 mm thickness. $CHCl_3$ and CCl_4 were of spectral purity (Uvasol, Merck). The concentration of the solution in $CHCl_3$ was *ca.* 4×10^{-3} mol dm^{-3}. In CCl_4 the concentrations were in the range between 10^{-4} and 4×10^{-4} mol dm^{-3}. For measurements in CCl_4 peak positions were determined with an accuracy of ± 0.2 cm^{-1} against polystyrene standard spectra.

NMR Spectra

The ^1H and ^{13}C NMR spectra were run for 0.1–0.2 M DMSO-d_6 solutions at 30 °C with a Bruker Avance DRX500 or DPX250 spectrometer working at 500.13 or 250.13 MHz for proton and 125.77 or 62.89 MHz for carbon-13, respectively.

^1H, ^{13}C and ^{15}N NMR chemical shift assignments are based on PFG ^1H, ^{13}C HMQC,[21,22] ^1H, ^{13}C HMBC[23] and ^1H, ^{15}N HMBC experiments. The detailed lists of the acquisition and processing parameters are available from E. K. on request.

Mass spectra

The low-resolution EI mass spectra were obtained by using a VG 7070E mass spectrometer (Manchester, UK) at 70 eV (direct insertion probe, ion source temperature 160 °C). Elemental compositions of fragment ions were determined using a VG ZabSpec instrument within an average accuracy of *ca.* 3×10^{-4} u based on accurate mass measurements at a resolution of 10 000–12 000 (10% valley definition) by the peak matching technique, using perfluorokerosene (PFK) as a reference compound. Metastable ion spectra (B/E and B^2/E linked scan technique, decompositions in the 1FFR) were recorded with the VG ZabSpec mass spectrometer.

Conclusions

The synthesis of a series of arylthiazolones with potential biological activity was described. The molecular as well as electronic structure of these compounds was characterised by means of spectroscopic (IR, NMR, MS) and theoretical (semiempirical and *ab initio*) calculations. Infrared spectroscopy shows that compounds **3** exist in solution mainly as lactam tautomers, either in free or hydrogen-bonded dimeric forms. Especially in concentrated $CHCl_3$ solution the hydrogen-bonded dimers and/or complexes with the solvent are the dominant species. As indicated by good linear correlations with Hammett σ values and AM1 C=O bond orders, the carbonyl stretching frequency of the monomeric species is quite sensitive to the effects of the substituents of the aryl ring. Transmission of such effects appears to be rather efficient. Similarly, correlations of Mulliken populations with the respective ^1H and/or ^{13}C NMR chemical shifts indicate that the carbon atom C5 is rather susceptible to effects of 4-aryl substituents. It is also evident that transmission of substituent effects to the C=O group takes place *via* this atom. Finally, aided by semiempirical molecular orbital calculations of the complete reaction paths (transition states and intermediates), a detailed description of the mass spectrometric fragmentation behaviour of 4-arylthiazol-2(3*H*)-ones is deduced.

Acknowledgements

The authors wish to thank The Finnish Academy (Grant no. 4284) and the Scientific Grant Agency of the Ministry of Education of the Slovak Republic (Grant no. 1/4000/97) for financial support.

References

1 (*a*) A. Dondoni and P. Merino, in *Comprehensive Heterocyclic Chemistry II*, Elsevier Science Ltd., 1st edn., 1996, vol. 3, pp. 373–474; (*b*) N. Ergenc and G. Capan, *Farmaco, Ed. Sci.*, 1994, **49**, 133; (*c*) V. Sutoris, A. Gaplovsky and V. Sekerka, *Chem. Pap.*, 1993, **47**, 260; (*d*) A. Cimirri, S. Grasso, A.-M. Monforte, P. Monforte and M. Zappala, *Farmaco, Ed. Sci.*, 1991, **46**, 817 and 925; (*e*) H. Naumann, H. Dehne, C. Fieseler, K. Goetzschel, M. Pallas, D. Schoenfelder, W. Mueller, W. Kochmann, K. Naumann and W. Steinke, Ger. (East) DD 241 844/1985/1987 (*Chem. Abstr.*, 1987, **107**, 91 901); (*f*) H. Hoelzel, H. Dehne, C. Fieseler, W. Kochmann, P. Krey, K. Naumann, K. Pede and M. Wind, Ger. (East) DD 200 402/1981/1983 (*Chem. Abstr.*, 1983, **99**, 153 858); (*g*) K. S. Dhami, S. S. Arora and K. S. Narang, *J. Org. Chem.*, 1962, **27**, 2147.

2 R. Dyckerhoff, *Ber. Dtsch. Chem. Ges.*, 1877, **10**, 119.

3 L. Arapides, *Justus Liebigs Ann. Chem.*, 1888, **249**, 7.

4 S. P. Cornwell, P. T. Kaye, A. G. Kent and G. D. Meakins, *J. Chem. Soc., Perkin Trans. 1*, 1981, 2340.

5 Y. Sanemitsu, S. Kawamura and Y. Tanabe, *J. Org. Chem.*, 1992, **57**, 1053.

6 D. S. Bariana, H. S. Sachdev and K. S. Narang, *J. Indian Chem. Soc.*, 1955, **32**, 427.

7 J. Teller, Habilitation Thesis, University of Rostock, Germany, 1988, pp. 41, 155.

8 J. Liebscher, in *Houben-Weyl, Methoden der Organischen Chemie*, Thieme Verlag, Stuttgart–New York, 4th edn., 1994, vol. E 8b, p. 153.

9 J. Teller, H.-J. Holdt and H. Dehne, *Z. Chem.*, 1989, **29**, 446.

10 For comparable correlative studies see: (*a*) A. Perjéssy, D. Rasala, D. Loos and D. Piorun, *Monatsh. Chem.*, 1997, **128**, 871; (*b*) Hu Geng Yuan, Ye Hua Hua, P. Koiš, N. Prónayová, Liu Quing and A. Perjéssy, *Heterocycl. Commun.*, 1998, **4**, 39; (*c*) E. Kolehmainen, K. Lappalainen, A. Perjéssy, M. Lácová and W. M. F. Fabian, *Magn. Reson. Chem.*, 1998, **36**, 511; (*d*) A. Perjéssy, K. Bowden, W. M. F. Fabian, O. Hritzová, N. Prónayová, Z. Šusteková and A. Al. Najjar, *Monatsh. Chem.*, 1999, **130**, 515 and references therein.

11 C. Hansch and A. Leo, *Substituent Constants for Correlation Analysis in Chemistry and Biology*, Wiley, New York, 1979.

12 J. J. P. Stewart, MOPAC 6.0, QCPE No. 455, Indiana University, Bloomington, IN.

13 A. Perjéssy and J. B. F. N. Engberts, *Monatsh. Chem.*, 1995, **126**, 871.

14 J. B. F. N. Engberts, G. R. Famini, A. Perjéssy and L. Y. Wilson, *J. Phys. Org. Chem.*, 1998, **11**, 261.

15 M. J. S. Dewar, E. G. Zoebisch, E. F. Healy and J. J. P. Stewart, *J. Am. Chem. Soc.*, 1985, **107**, 3902.

16 J. J. P. Stewart, *J. Comput. Chem.*, 1989, **10**, 209 and 221.

17 T. Clark, VAMP, Erlangen Vectorized Molecular Orbital Package, Version 4.40, Computer-Chemie-Zentrum, University Erlangen-Nürnberg, Germany, 1992.

18 J. Baker, *J. Comput. Chem.*, 1986, **7**, 385.

19 M. J. Frisch, G. W. Trucks, H. B. Schlegel, P. M. W. Gill, B. G. Johanson, M. A. Robb, J. R. Cheeseman, T. Keith, G. A. Pepersson, J. A. Montgomery, K. Raghavachari, M. A. Al-Lahm, V. G. Zakrzewski, J. V. Ortiz, J. B. Foresman, C. Y. Peng, P. Y. Ayala, W. Chen, M. W. Wong, J. L. Andres, E. S. Replogle, R. Gomperts, R. L. Martin, D. J. Fox, J. S. Binkley, D. J. Defrees, J. Baker, J. J. P. Stewart, M. Head-Gordon, C. Gonzales and J. A. Pople, Gaussian 94, Revision B. 3, Gaussian, Inc., Pittsburgh, 1993.

20 J. A. Pople, A. P. Scott, M. W. Wong and L. Radom, *Isr. J. Chem.*, 1993, **33**, 345.

21 A. Bax, R. H. Griffey and B. L. Hawkins, *J. Magn. Reson.*, 1983, **55**, 301.

22 A. Bax and S. Subramanian, *J. Magn. Reson.*, 1986, **67**, 565.

23 A. Bax and M. F. Summers, *J. Am. Chem. Soc.*, 1986, **108**, 2093.